

Comprehensive Microarray Analysis Identify Dysregulated MicroRNAs in Pressure Overload Affected Hearts

Eskildsen TV^{1,2}
Schneider M²
Zhai P³
Sandberg MB²
Knudsen LA¹
Andersen DC^{1,2}
Sadoshima J³
Sheikh SP^{1,2*}

Abstract

Background: MicroRNAs (miRNAs) are emerging as key regulators of cardiovascular development and disease, being involved in cardiac hypertrophy, fibrosis, remodeling and heart failure. Aortic stenosis is the most common valvular heart disease, and thus, we undertook a detailed analysis of differentially expressed miRNAs in this disease.

Methods and Findings: We set up a model of aortic stenosis by performing transverse aorta constriction (TAC) in adult mice resulting in a rapid increase in left ventricle pressure load, pronounced hypertrophy, initiated fibrosis, impaired ejection performance and dysfunctional diastole. Using miRNA microarray we then identified more than 300 differentially regulated miRNAs in the hearts of mice affected by aortic stenosis. Five of these were validated using qRT-PCR in which miR-21 and miR-208b were striking because of their substantial 2-4 fold increase at day 21 post TAC when compared with the control group. Furthermore, we identified three novel miRNAs (miR-24, miR-301a and miR-335) that were highly induced in transverse aorta constricted mice compared to SHAM operated mice. Interestingly, the increased expression of miR-24, miR-301a and miR-335 in TAC affected hearts were not found in an animal model of myocardial infarction.

Conclusion: These data suggests that the novel miRNAs are regulated in the heart specific to aortic stenosis, and may serve as biomarker candidates for future diagnosis, prognosis or treatment.

Keywords: Aorta stenosis; Transverse aorta constriction; Hypertrophy; Fibrosis; Echocardiography; MicroRNA

- 1 Department of Cardiovascular and Renal Research, J.B. Winslowvej 21 3., University of Southern Denmark, DK-5000 Odense, Denmark
- 2 Department of Clinical Biochemistry and Pharmacology, Sdr. Boulevard 29, Odense University Hospital, DK-5000 Odense, Denmark
- 3 Department of Cell Biology and Molecular Medicine, 185 South Orange Ave., University of Medicine and Dentistry of New Jersey, Newark, NJ 07103, USA

***Corresponding author:**
Sheikh SP

✉ soeren.sheikh@rsyd.dk

Department of Clinical Biochemistry and Pharmacology, Sdr. Boulevard 29, Odense University Hospital, DK-5000 Odense, Denmark

Tel: +45 65414468

Introduction

Cardiovascular disease affecting more than 1 billion people worldwide, has long been the leading cause of death [1]. Cardiac hypertrophy and fibrosis, the common pathological responses to many cardiovascular diseases such as myocardial infarction, hypertension and valvular heart diseases, are major determinants of mortality and morbidity [2]. Cardiovascular disease can arise from increased pressure overload caused by essential hypertension or aortic stenosis. Aortic stenosis is the most prevalent of all valvular heart diseases and is characterized by narrowing of the aortic orifice resulting in left ventricular pressure overload, cardiac hypertrophy and fibrosis

[3]. Furthermore pressure overload increases left ventricular afterload thereby impairing cardiac ejection performance [3]. Transverse aortic constriction (TAC) in the mouse is a commonly used experimental model for pressure overload-induced cardiac hypertrophy and heart failure. TAC initially leads to compensated hypertrophy of the heart, which is often associated with a temporary enhancement of cardiac contractility. Over time, however, the response to the chronic hemodynamic overload becomes maladaptive, resulting in cardiac dilatation and heart failure.

MicroRNAs (miRNAs) have recently been found to constitute a novel layer of regulation on cardiac disease, hypertrophy and fibrosis [4-7]. Hence, dysregulated miRNAs have been suggested

as biomarkers and novel drug targets in cardiovascular diseases, although clinical testing has yet to be initiated [8,9]. Cardiac cell growth being the key cellular event in formation of cardiac hypertrophy, we hypothesized that miRNA expression pattern in pressure overload-induced hypertrophic hearts may be different than in healthy hearts.

MicroRNAs are small non-coding RNAs that regulate a substantial fraction of the genome by binding to the 3' untranslated region (3'UTR) of target mRNAs [10]. The mammalian miRNAs are highly conserved, and each miRNA is predicted to target hundreds of target mRNAs [11]. Theoretically, these miRNAs are ideally suited to co-regulate gene expression events in cellular responses to diseases such as pressure overload and left ventricular hypertrophy. Several miRNAs are known to be aberrantly expressed in cardiac diseases, in particular miR-21, miR-29, miR-133a and miR-208b [4-7,12-18]. For example, miR-21 has been reported as the most dysregulated miRNA in many cardiac pathologies and has increased expression in both failing, hypertrophic and fibrotic hearts [19-22]. In the present study we set up an animal model of aortic stenosis and examined the injury affecting the heart during the 21 days of transverse aorta constriction (TAC). We investigated the miRNA expression in the left ventricles of these mice and expanded these results to data concerning myocardial infarction (MI) in a mouse model. We identified more than 300 progressively changing miRNAs during the period of 21 days. From these data, miR-24, miR-301a and miR-335 were suggested to be specifically involved in development of cardiac hypertrophy and remodeling following TAC.

Materials and Methods

Transverse aorta constriction (TAC)

All animal experiments were approved by Institutional Animal care and Use Committee of the University of Medicine and Dentistry of New Jersey (#11005).

To determine the expressional changes of miRNA in pressure overloaded hearts, we applied a mouse aortic stenosis model by transverse aortic constriction (TAC). In brief, 12 week old female C57/BL6 mice were anesthetized IP with a mixture of Ketamine (100 mg/kg) and Xylazine (5 mg/kg). The animals were ventilated via tracheal intubation connected to a MiniVent (Harvard Apparatus) with a tidal volume 0.2 ml and a respiratory rate of 100 breaths per minute. Under sterile conditions, the chest was opened at the second intercostal space and the thymus glands were superiorly reflected. The thoracic aorta was dissected and a 7-0 prolene suture tied around the aorta between right and left common carotid artery against a blunted 26-gauge needle (**Figure 1**). Age matched control mice underwent a sham operation involving thoracotomy and aortic dissection, without constricting the aorta. From 12 mice that underwent TAC or SHAM surgery for each time point (72 mice), 10 mice were included in the control group (day 0), 9, 8, 10, 12 and 11 mice were included in day 1, 4, 7, 14 and 21 respectively.

Ligation of left anterior descending (LAD) coronary artery

All animal experiments were approved by the Danish National

Animal Experiment Inspectorate (Permission # 2009/561-1663 (TAC) and # 2011/561-1966 (LAD)).

To study if the expressional changes of miRNA are specific to the TAC hearts we applied a myocardial infarct (MI) mouse model of ligation of left anterior descending (LAD) coronary artery, causing myocardial infarct MI in the area close to the ligated artery. The surgery was performed as described above with some minor modifications. Under sterile conditions, the chest was opened at the 4th intercostal space and the LAD coronary artery dissected and a 7-0 prolene suture tied and closed around the artery. Age matched control mice underwent a sham operation. No control group (day 0) was present in this study and data are presented as pooled data from 2, 4, 2, 1 and 4 mice at day 2, 4, 7, 14 and 28 after LAD respectively. One or two pooled SHAM mice were included at each time point. Altogether 21 mice were used in the study.

Echocardiography

Mice were anesthetized IP with 2.5% avertin (0.010-0.015 ml/g). Transthoracic echocardiography (Sequoia C256; Acuson, Mountain View, CA) was performed using a 13-MHz linear ultrasound transducer. The chest was shaved, mice placed on a warm saline bag in a left lateral position and warm coupling gel applied to the chest. Electrocardiographic leads were attached to each limb using needle electrodes. Two-dimensional image and M-mode tracing (sweep speed=100-200 mm/s) were recorded from parasternal short-axis view at the mid papillary muscle level. The images were recorded as videotape and freeze frames were analyzed using the Adobe Photoshop CS5. M-mode measurements of left ventricle (LV) internal diameter and wall thickness were made from three consecutive beats. End-diastolic measurements were taken at the time of the apparent maximal LV diastolic dimension. End-systolic measurements were made at the time of most anterior systolic excursion of the posterior wall (**Figure 1**). Left ventricular fractional shortening (FS) was calculated as $(d-s)/d$, where d and s represents LV end dimensions of diastole and systole respectively. Similarly ejection fraction (EF) was calculated by the cubed method as follows $(d^3-s^3)/d^3$.

Hemodynamic measurements

At the day of sacrifice the mice underwent hemodynamic measurements using a 1.4-French (Millar Instruments) catheter-tip micromanometer catheter. The mice were anesthetized IP with a mixture of Ketamine (100 mg/kg) and Xylazine (5 mg/kg). The catheter was inserted through the right carotid artery into the aorta and then into the LV and in the femoral artery wherein pressure was measured. Mice with pressure gradients below 30 or above 90 were excluded from the following analysis.

After sacrificing the mice, hearts were dissected under sterile conditions and sectioned into atria, right ventricle and left ventricle used for RNA isolation or cryopreserved for immunohistochemistry.

Sirius red staining

Fibrosis was identified by Sirius Red Staining for collagen deposits. Cryosections were equilibrated at room temperature for 30 min,

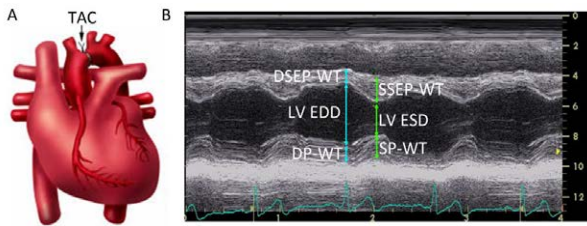


Figure 1 Schematic presentation of transverse aortic constriction operated heart and M-mode echocardiogram. A) TAC in the mouse is a commonly used experimental model for pressure overload induced cardiac hypertrophy and heart failure. A suture is placed between right and left carotid arteries against a piece of 26 gauge blunt needle. B) Normal representative M-mode measurements of left ventricle internal diameter and wall thickness. TAC: Transverse Aortic Constriction, DSEPWT: Diastolic Septal Wall Thickness, LVEDD: Left Ventricle End Diastolic Diameter, DPWT: Diastolic Posterior Wall Thickness, SSEPWT: Systolic Septal Wall Thickness, LVESD: Left Ventricle End Systolic Diameter, SPWT: Systolic Posterior Wall Thickness.

rinsed in a mixture of normal buffered formalin (NBF) (37%) and ethanol (93%) for 45 sec, rehydrated (5 min), and subsequently counterstained (15 min) with Weigert's Iron Hematoxylin (Sigma-Aldrich, HT-107/109). Following a wash, sections were further incubated (60 min) with 0.1% Sirius red (Sigma-Aldrich, P6744) in saturated picric acid (Sigma-Aldrich, 365548), and finally washed twice in 99% ethanol. Sections were mounted with Pertex and analyzed by bright-field microscopy using a Leica DML332 equipped with a Leica DFC300F camera.

Microarray and data processing

The miRNA expression profiling was performed as two-color common reference hybridizations on LNA based arrays (miRCURY LNA™ microRNA Array ready to spot probe set, Exiqon, Denmark) spotted in-house on CodeLink™ HD Activated slides (DHD1-0023, SurModics, Eden Prairie, MN) according to manufacturer's recommendation. Samples were labeled with Hy3 and the common reference (pool of all samples) was labeled with Hy5, by use of miRCURY LNA microRNA Array Power labeling kit (208032-A, Exiqon) and hybridized for 16 hours. Slides were washed (208021, Exiqon), scanned on an Agilent (G2565CA) Microarray scanner and analyzed by the Genepix 6.0 software. Normalization and background correction was performed with "R" software using the "vsN" package (Bioconductor), and quadruplicate spots were averaged. Differential expression was assayed using the "limma" package (Bioconductor) by fitting the eBayes linear model and contrasting individual treatments with untreated controls. Log₂ fold changes were calculated using the top table function of the limma package.

mRNA and miRNA analysis

Relative qRT-PCR of mRNA and miRNA were performed as previously described [23,24]. Briefly, total RNA was extracted using TriReagent protocol (Molecular Research Center, Inc.), and RNA purity, integrity and quantity was examined by nanodrop

(Nanodrop® Technologies) and Bioanalyzer (Agilent 2100) measurements. Relative quantitative mRNA PCR was performed on reverse transcribed cDNA (High Capacity cDNA RT kit; Applied Biosystems) using primers listed in **Table S1**. For miRNA qRT-PCR primers specific for mice miR-21 (#000397), miR-24 (#000402), miR-208b (#002290), miR-301a (#000528), miR-335 (#000546) and let-7i (#002221) were purchased from Applied Biosystems. Amplification and detection were performed using 7900HT Fast Real-Time PCR System (Applied Biosystems). As recommended by others [25,26] and previously described [23,24] we used the qBase+ software to normalize all qRT-PCR data against stably expressed control genes (**Table S2**).

Statistical analysis

Results are represented as mean±s.d. except for LAD experiments, in which pooled data was used. All analyses comprised independent experiments, and one-way ANOVA or two-way ANOVA were performed as indicated (GraphPad Prism (version 5.0) software) to test significant levels. Differences were considered to be significant at $P < 0.05$. Number of animals used and statistical method for each analysis is described in figure or table text.

Results

Pressure overload, cardiac hypertrophy and fibrosis are sustained in the mice model

Initially, we confirmed successful aortic constriction by measuring the pressure gradient across the constricted area using two Millar catheters. Constriction resulted in a stable and significant elevated pressure overload of 55 ± 17 mmHg ($P < 0.001$, $n=7$) (**Table 1**). Furthermore, the TAC mice exhibited pronounced cardiac hypertrophy as evidenced by a significant 33% increased left ventricle to body weight ratio ($P < 0.001$, $n=7$) at day 21 post TAC versus SHAM operated mice ($n=4$). The mass of the left ventricle increased from 83 ± 6 mg ($n=10$) in control mice to 117 ± 22 mg ($n=7$) in the TAC mice ($P < 0.05$). Left ventricular hypertrophy was further validated by a significantly higher expression level of *B-type natriuretic peptide (BNP)* ($P < 0.01$) and *β-myosin heavy chain (β-MHC)* ($P < 0.01$) (**Figure 2A**). Development of cardiac fibrosis during the time period was confirmed by a significant increase in the fibrosis related genes *α-smooth muscle actin (α-SMA)* ($P < 0.001$) and *matrix metalloproteinase 2 (MMP2)* ($P < 0.05$), and a clear tendency for upregulation of *Procollagen-1* and *Fibronectin* (**Figure 2A**). Similar to collagen gene expression, the visualization of collagen deposition in the left ventricles of TAC mice was variable (**Figure 2B**).

Echocardiography

Physiological measurements obtained using echocardiography confirmed hypertrophic and dysfunctional hearts in TAC operated mice compared to SHAM mice. TAC affected mice exhibited dilative remodeling of the left ventricles as evidenced by a significantly increased diastolic septal wall thickness (DSEPWT), diastolic posterior wall thickness (DPWT) and left ventricle end diastolic diameter (LV-EDD) ($P < 0.05$, $n=7$) compared to SHAM operated mice ($n=3-4$) (**Table 1**). In systole, the septal wall thickness (SSEPWT), the posterior wall thickness (SPWT) and the left ventricle end systolic dimension (LVESD) ($n=7$) were increased

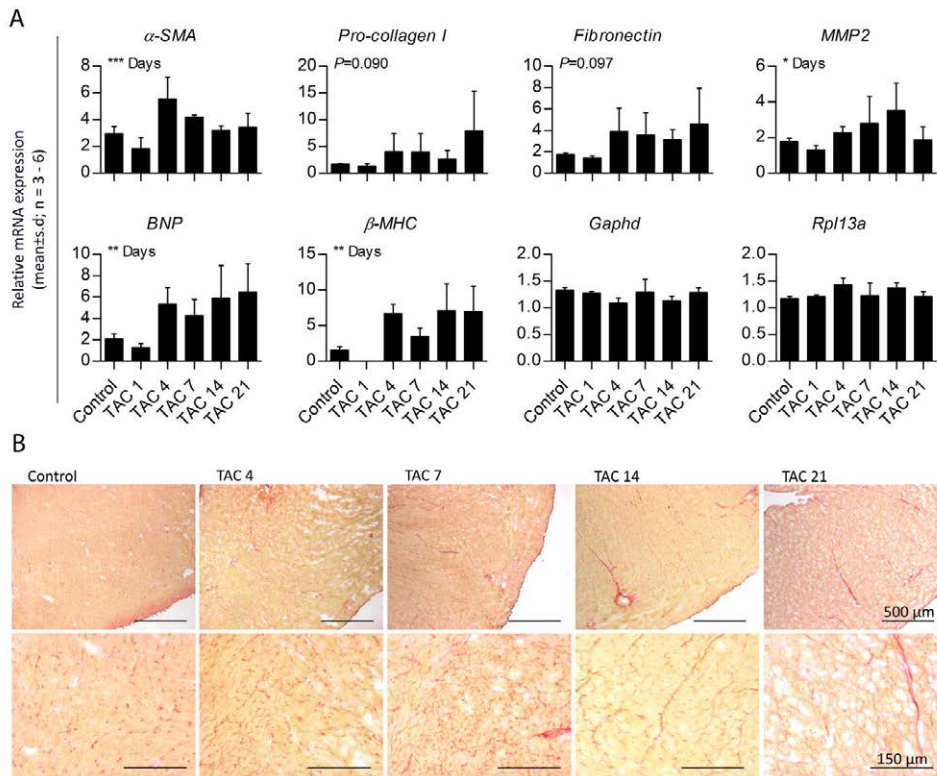


Figure 2 Characterization of TAC effect on left ventricles. A) Representative sections of left ventricles of TAC hearts stained with Sirius Red for collagen deposition. The control section has unspecific staining in the border, which may be due to technical difficulties. B) qRT-PCR for fibrotic markers; α -SMA, Fibronectin, Procollagen-I and MMP2 and for the early and late marker of hypertrophy, BNP and β -MHC normalized to two stably expressed reference genes. Reference genes used for normalization, M and CV values is available in Table S2. Data is presented as mean \pm s.d, n=3-6. Statistical significance was tested by One-way ANOVA for significant difference over the period *P<0.05, **P<0.01 and ***P<0.001.

non-significantly in TAC operated mice as compared to SHAM operated mice (Table 1). Additionally the percentage of ejection fraction and fractional shortening were significantly decreased in aortic constricted mice ($P<0.01$, n=7) versus SHAM mice (n=3-4) indicating decreased myocardial contractility (Table 1). Positron Emission Tomography (PET) analysis was performed to confirm dysfunctional hearts in LAD operated mice compared to SHAM mice. The PET-scan clearly showed dilative remodeling of the hearts as evidenced by ejection fraction (EF) and diastolic volume (EDV) and end systolic volume (ESV). Data not shown.

Constriction mediated pressure overload regulates more than 300 microRNAs in the heart

We performed miRNA microarray and found more than 335 miRNAs identified as significantly altered ($P<0.05$) in at least one of the five time points in the left ventricles of TAC affected mice (n=3) compared to control mice at day 0 (n=3) (Table S3). Of the 335 miRNAs differentially regulated in TAC operated mice, miR-21 and miR-208b, which are known to be involved in numerous cardiac diseases, were the most up-regulated and thus used as positive controls in our analysis (Figure 3A).

By selecting the 10 most significantly regulated miRNAs from each time point, we reduced the miRNA list to include the 38 most

significantly altered miRNAs (Table 2). Interestingly, two novel miRNAs together with miR-24, which has not been described in detail, were selected based on differential expression during the time line (Figure 3). MiR-24 was significantly elevated at the late time points by 1.17 and 1.27 fold at day 14 and day 21 respectively (Table 2). The miR-301a was significantly increased at day 7 (1.24 fold) and continued to be increased at day 14 (1.47 fold) and 21 (1.47 fold) (Table 2), whereas miR-335 was peaking at day 14 (2 fold) and rapidly declined hereafter (Table 2). To confirm these results we performed qRT-PCR of the five miRNAs (miR-21, -208b, -24, -301a and -335) (Figure 3A). Additionally miR-24, miR-301a and miR-335 were compared to miRNA expression levels in SHAM operated mice wherein no regulation of the miRNAs was observed (Figure 3B).

MiR-24, miR-301a and miR-335 regulation in response to myocardial infarction

The TAC model has been used to define changes occurring during hypertrophy such as cell size, gene and miRNA expression and incidence of apoptosis [27]. However other models of hypertrophy and heart failure, such as the MI model, have been extensively studied. MI leads to scar formation and left ventricular remodeling, including cardiac dilatation, contractile dysfunction,

Table 1 Pathological measurements and Echocardiographic analysis of TAC and SHAM operated mice.

	Day 0 Control	Day 4		Day 7		Day 14		Day 21		Two-way ANOVA
		SHAM	TAC	SHAM	TAC	SHAM	TAC	SHAM	TAC	
BP aorta (mmHg)	70.0 ± 15.0		120.3 ± 2.5		106.8 ± 8.9	83.5 ± 5.2	133.6 ± 17.6	82.4 ± 20.7	136.1 ± 16.9	*** TAC (one-way)
BP F. artery (mmHg)	68.0 ± 10.5		68.1 ± 4.7		66.8 ± 8.7	86.5 ± 22.9	71.0 ± 6.3	82.5 ± 15.6	74.6 ± 9.9	^{ns} TAC (one-way)
ΔP (mmHg)	2.0 ± 3.5		52.2 ± 4.8		40.0 ± 10.1	-3.0 ± 25.6	62.6 ± 16.7	-0.1 ± 6.8	61.5 ± 19.0	*** TAC ** Days
LV/BW (mg/g)	3.8 ± 0.3	3.6 ± 0.3	4.0 ± 0.5	3.7 ± 0.2	4.4 ± 0.5	3.3 ± 0.2	4.1 ± 0.5	4.3 ± 0.2	5.1 ± 1.0	*** TAC *** Days
LV/TB (mg/mm)	4.8 ± 0.4	4.3 ± 0.3	5.4 ± 1.0	4.4 ± 0.4	5.3 ± 0.3	4.0 ± 0.3	5.4 ± 0.8	4.7 ± 0.3	6.5 ± 1.1	*** TAC ** Days
DSEPWT (mm)	0.6 ± 0.1	0.7 ± 0.2	0.7 ± 0.1	0.5 ± 0.04	0.6 ± 0.1	0.6 ± 0.2	0.7 ± 0.1	0.6 ± 0.04	0.8 ± 0.1	* TAC ** Days
LV-EDD (mm)	4.2 ± 0.3	4.3 ± 0.3	3.8 ± 0.2	4.3 ± 0.04	4.0 ± 0.1	4.1 ± 0.4	4.0 ± 0.2	4.4 ± 0.3	4.2 ± 0.3	* TAC ^{ns} Days
DPWT (mm)	0.5 ± 0.1	0.6 ± 0.1	0.6 ± 0.1	0.4 ± 0.04	0.6 ± 0.04	0.6 ± 0.2	0.6 ± 0.1	0.5 ± 0.1	0.7 ± 0.1	* TAC * Days
SSEPWT (mm)	0.8 ± 0.1	0.9 ± 0.1	0.9 ± 0.1	0.7 ± 0.1	0.8 ± 0.1	0.8 ± 0.2	0.9 ± 0.1	0.9 ± 0.2	1.0 ± 0.1	^{ns} TAC * Days
LV-ESD (mm)	3.1 ± 0.3	3.3 ± 0.1	3.0 ± 0.3	3.2 ± 0.1	3.0 ± 0.1	3.1 ± 0.4	3.2 ± 0.3	3.3 ± 0.4	3.4 ± 0.3	^{ns} TAC ^{ns} Days
SPWT (mm)	0.8 ± 0.1	0.8 ± 0.1	0.8 ± 0.1	0.7 ± 0.02	0.7 ± 0.1	0.8 ± 0.3	0.8 ± 0.1	0.8 ± 0.1	0.9 ± 0.2	^{ns} TAC ^{ns} Days
FS (%)	26.7 ± 2.1	23.0 ± 2.9	22.4 ± 3.2	24.8 ± 1.8	24.8 ± 1.7	25.7 ± 3.8	21.2 ± 3.3	25.0 ± 3.8	18.1 ± 1.9	** TAC *** Days
EF (%)	60.5 ± 3.4	54.2 ± 5.1	53.1 ± 5.5	57.4 ± 3.1	57.3 ± 2.9	58.8 ± 6.0	50.9 ± 6.1	57.6 ± 6.6	44.9 ± 16.3	** TAC *** Days
HR (bpm)	385 ± 46	419 ± 8	470 ± 29	406 ± 42	428 ± 26	422 ± 18	435 ± 25	443 ± 43	405 ± 54	^{ns} TAC ** Days
Number (n)	10	3	4-5	4	4-6	4	6-8	4	5-7	

BP: Blood Pressure, F. artery: Femoral Artery, ΔP: trans-systolic pressure gradient, LV/BW and LV/TB: left ventricle weight ratio to body weight or Tibia length, DSEPWT and SSEPWT: Diastolic and Systolic Septal Wall Thickness, LVEDD and LVESD; Left Ventricular End-Diastolic and End-Systolic dimension, DPWT and SPWT: Diastolic and Systolic Posterior Wall Thickness. FS (Fractional Shortening) and EF (Ejection Fraction) are represented as percentage. HR: Heart Rate. Boldface marks significantly altered values. Data are shown as mean ± s.d. Statistical significance was tested by One-way or Two-way ANOVA and treatment effects were assessed by Bonferroni post test, n=3-10 as indicated in the table. *P<0.05, **P<0.01 and *** P<0.001

cardiomyocyte hypertrophy and fibrosis [28]. However to examine whether the regulation of miR-24, 301a and -335 is specific for the aortic stenosis model, we examined the effects of MI in mice with coronary artery ligation. In contrast to the TAC mice, the MI mice suffer from ischemia in the area close to the ligation [29]. Here, we did not observe a regulation of miR-24, miR-301a and miR-335 expression in MI affected mice compared to the corresponding SHAM operated mice (**Figure 3C**) indicating interestingly, that regulation of miR-24, miR301a and miR-335 is specific to TAC affected mice.

In summary, we identified expressional changes of more than 300 miRNAs through a timeline of 21 days in mouse hearts affected by TAC. We validated the differential expression of miR-24, -301a and -335 in the left ventricle of TAC mice compared to SHAM operated mice (**Figure 3A**) and found this miRNA regulation to be

specific for aortic stenosis and suggestively not part of a general cardiac disease response.

Discussion

The molecular mechanisms underlying left ventricular pressure overload and cardiac hypertrophy involves a change in the gene expression profile which recapitulates the neonatal growth phenotype. This mostly includes the upregulation of translation- and transcription-related genes, including miRNAs [16-18,30,31]. We performed constriction of aorta in mice over a period of 21 days resulting in a clear and sustained pressure overload affecting the left ventricles, leading to hypertrophic and fibrotic changes, dilative remodeling and decreased ejection performance of the affected hearts.

In these settings we identified altered regulation of multiple

miRNAs in left ventricles of mice affected by the pathological condition of aortic stenosis. In specific, we identified two novel miRNAs, miR-301a and miR-335 together with miR-24 which previously has been identified in cardiac disease, but not been described in detail [6,29,32]. Additionally we found altered expression of several well-described cardiac disease miRNAs including miR-21, miR-29, miR-133a and miR-208b [4-7,12], all confirming our methodological setup.

MiR-24 was identified in the left ventricles of our TAC model steadily increasing during the timeline. Comparable to this, van Rooij et al. have previously described two animal models of hypertrophy *in vivo* (TAC mice and transgenic mice expressing activated calcineurin A (CnA)) and found increased expression of miR-24 in both models. They describe that miR-24 induce myocyte hypertrophy *in vitro* [6]. Furthermore, when overexpressing miR-24 specifically in the heart under the control of the α -MHC promoter, no offspring was obtained suggesting that overexpression of miR-24 causes embryonic lethality [6]. We further examined the expression of miR-24 in whole hearts of MI mice and did not find any regulation of miR-24. However, we cannot exclude that miR-24 would be regulated in MI mice comparable to TAC mice if we examined the left ventricles alone. In addition to this, miR-24 has been found as regulated in mice hearts following myocardial infarction. One study identified miR-24 as considerably increased in endothelial cells affected by MI [29]. Here, miR-24 was found to induce endothelial cell apoptosis and abolish new formation of vasculature by targeting the endothelium-enriched transcription factor (GATA2) and the p21-activated kinase (PAK4) [29]. Oppositely, a recent study revealed a contrary role of miR-24 in cardiomyocyte apoptosis [32], showing that miR-24 is decreased in the border zone after MI. In the recent study, restored levels of miR-24 reduce myocyte apoptosis, infarct size and cardiac dysfunction by targeting Bim [32]. These different results might be caused by cell specificity as opposite results were found in endothelial cells and myocytes respectively. We used the whole cell fraction from homogenized hearts of MI mice, which might equalize the differential expression in different cell types.

Even more excitingly, miR-24 has been identified as upregulated in human aortic stenosis patients [18], indicating that altered expression of miR-24 is not only a spurious factor found in mice, but may also play a role in the hearts of patients affected by aortic stenosis.

The miR-335 has not previously been described in the heart, however miR-335 is reported as a regenerative miRNA induced in muscular dystrophy patients and in a muscular dystrophy mice model [33]. The increased expression of miR-335 in muscular dystrophy is found in both whole gastronemius muscles and in isolated and newly formed myofibers during post-ischemic regeneration [33]. Moreover miR-335 has been shown to be upregulated in myoblast differentiation *in vitro* [33]. This miRNA is increasing and decreasing in the muscular dystrophy mice model, in the same manner as in our

TAC model, peaking at day 14 and declining at day 21, suggesting that miR-335 in the left ventricles of mice affected by aortic stenosis could be involved in similar regenerative process as in muscular dystrophy.

MiR-301a is not well-described and has not previously been identified in cardiac diseases. A few studies, however, reported that miR-301a is involved in diverse cancers [34,35]. As with miR-24, neither miR-301a nor miR-335, were regulated in hearts affected by MI.

In agreement with others, we identified miR-29 as significantly downregulated at day 7 and 14 post TAC [13-15] and miR-133 was significantly increased at day 14 post TAC in our study [16-18]. However neither miR-29a nor miR-133a were among the 10 most significantly regulated miRNA at any of the time points and thus not validated in our study. Moreover, we identified miR-21 and miR-208b as the two most up-regulated miRNAs at day 21 post TAC. The role of miR-21 in cardiomyocytes and fibroblasts are heavily debated. Most studies find an induction of myocardial hypertrophy and fibrosis by miR-21 [19,20] whereas others suggest an anti-hypertrophic effect of miR-21 in isolated cardiomyocytes [21,22]. As described, miR-208b has been reported to play a role in re-activation of the fetal gene program including increased β -MHC and decreased α -MHC, thus being protective against acute, but not chronic cardiac stress-induced remodeling [6].

In summary, we have for the first time identified altered expression of three novel miRNAs; miR-24, -301a and -335 in the left ventricle of TAC affected mice compared to controls and found that regulation of miR-24, miR-301a and miR-335 is specific for aorta stenosis affected mice and could not be found in mice with myocardial infarction. To date, the functional role of these three miRNAs has not been thoroughly investigated and it would be of great interest to search for targets and elucidate to which extent these miRNAs are involved in the developmental process of TAC induced hypertrophy.

Acknowledgment

We thank Shumin Gao, Tonja Lyngse Jørgensen and Charlotte Nielsen for excellent technical assistance.

Sources of Funding

This work was funded by the John and Birthe Meyer Foundation, The Danish Cardiovascular Academy, the Danish heart Association (R78-A2847), The Danish National Research Council (#09-073648), The Lundbeck Foundation and JS is funded by U.S. Public Health Service Grants and the Foundation of Leducq Transatlantic Network of Excellence.

Conflict of Interest

All authors declare no conflict of interest.

Table 2 (MicroArray) The 38 miRNAs listed in this table are the top 10 most significantly regulated miRNAs from each timepoint. The expression level is presented by average of three samples and as fold change to control. Boldface indicates significant differences from control ($P < 0.05$). miR-21, miR-24, miR-208b, miR-301a and miR-335 were selected for validation. For full list of all significantly regulated genes, see supplementary Table S3.

miRNA	TAC1		TAC4		TAC7		TAC14		TAC21	
	Fold	P								
miR-19a	0.99	0.882	0.99	0.781	1.05	0.225	1.14	0.004	1.21	<0.001
miR-21	1.07	0.750	1.41	0.139	1.32	0.222	1.47	0.102	3.71	<0.001
mmu-miR-21*	2.38	<0.001	0.91	0.393	1.03	0.806	0.90	0.340	1.28	0.033
miR-22	0.91	0.024	0.93	0.088	0.84	0.001	0.91	0.025	1.04	0.375
miR-24	1.00	0.922	1.04	0.312	1.11	0.023	1.17	0.002	1.27	<0.001
miR-26b*	0.89	0.010	0.89	0.010	0.84	0.001	1.00	0.966	0.98	0.646
miR-32*	1.31	0.002	1.08	0.269	1.10	0.178	1.09	0.215	1.04	0.609
mmu-miR-125b*	0.91	0.066	0.85	0.003	0.93	0.122	0.86	0.008	0.91	0.081
miR-135a	0.73	<0.001	0.78	<0.001	0.73	<0.001	0.84	0.008	0.95	0.330
miR-136*	0.81	0.023	0.72	0.001	0.79	0.014	0.89	0.176	0.84	0.049
miR-142-5p	0.98	0.892	1.16	0.243	1.70	0.001	1.21	0.145	1.55	0.003
miR-146a	1.06	0.358	0.99	0.939	1.12	0.113	1.29	0.002	1.30	0.002
miR-193a-3p	0.94	0.303	1.10	0.133	1.19	0.008	1.28	0.001	1.21	0.005
miR-200b*	0.90	0.022	0.86	0.002	0.86	0.002	0.97	0.507	0.98	0.532
miR-208b	1.32	0.079	1.40	0.036	1.30	0.090	1.74	0.002	2.08	<0.001
miR-301a	1.03	0.603	1.09	0.128	1.24	0.002	1.47	0.000	1.47	<0.001
miR-323-5p	0.78	0.155	0.49	0.001	1.09	0.598	0.75	0.112	0.77	0.146
mmu-miR-327	1.36	0.001	0.97	0.704	0.95	0.520	0.88	0.112	0.81	0.016
miR-335	1.05	0.689	1.01	0.953	1.26	0.094	1.97	<0.001	1.38	0.027
mmu-miR-455	1.01	0.902	1.10	0.107	1.22	0.002	1.27	0.001	1.34	<0.001
mmu-miR-465b-5p	1.15	0.003	1.00	0.917	0.94	0.153	0.87	0.004	0.86	0.002
mmu-miR-466d-5p	1.28	0.003	1.07	0.324	1.08	0.301	1.05	0.479	1.00	0.945
miR-505	0.98	0.906	0.82	0.355	0.72	0.122	0.50	0.001	0.94	0.782
miR-510	1.32	0.017	1.43	0.003	1.44	0.003	1.45	0.003	1.31	0.018
miR-511	0.88	0.233	0.75	0.016	0.65	0.001	0.89	0.302	0.80	0.055
miR-513-3p	1.05	0.233	1.11	0.021	1.10	0.031	1.16	0.002	1.26	<0.001
miR-518a-5p	1.05	0.308	1.17	0.002	1.13	0.011	1.04	0.345	1.13	0.009
miR-541*	0.83	0.138	0.73	0.020	0.62	0.002	0.79	0.072	0.77	0.047
miR-545	0.45	0.001	0.50	0.003	0.56	0.009	0.61	0.022	0.60	0.017
miR-548a-3p	0.90	0.020	0.87	0.004	0.86	0.003	0.93	0.106	0.95	0.234
miR-558	0.71	0.003	0.81	0.045	0.85	0.128	0.86	0.132	0.80	0.038
miR-620	1.15	0.023	0.90	0.013	0.86	0.001	0.96	0.253	0.89	0.010
miR-628-3p	0.94	0.475	0.85	0.071	0.71	0.001	0.83	0.036	0.75	0.003
miR-629*	1.10	0.038	1.20	0.001	1.17	0.002	1.10	0.027	1.26	<0.001
miR-637	2.89	<0.001	1.05	0.802	0.90	0.597	0.70	0.080	0.70	0.077
mmu-miR-666-5p	1.07	0.208	1.12	0.057	1.09	0.141	1.10	0.080	1.36	<0.001
mmu-miR-677	0.93	0.177	1.11	0.071	1.08	0.150	1.23	0.001	1.36	<0.001
mmu-miR-706	1.33	0.002	1.12	0.145	1.12	0.147	1.04	0.624	1.11	0.200

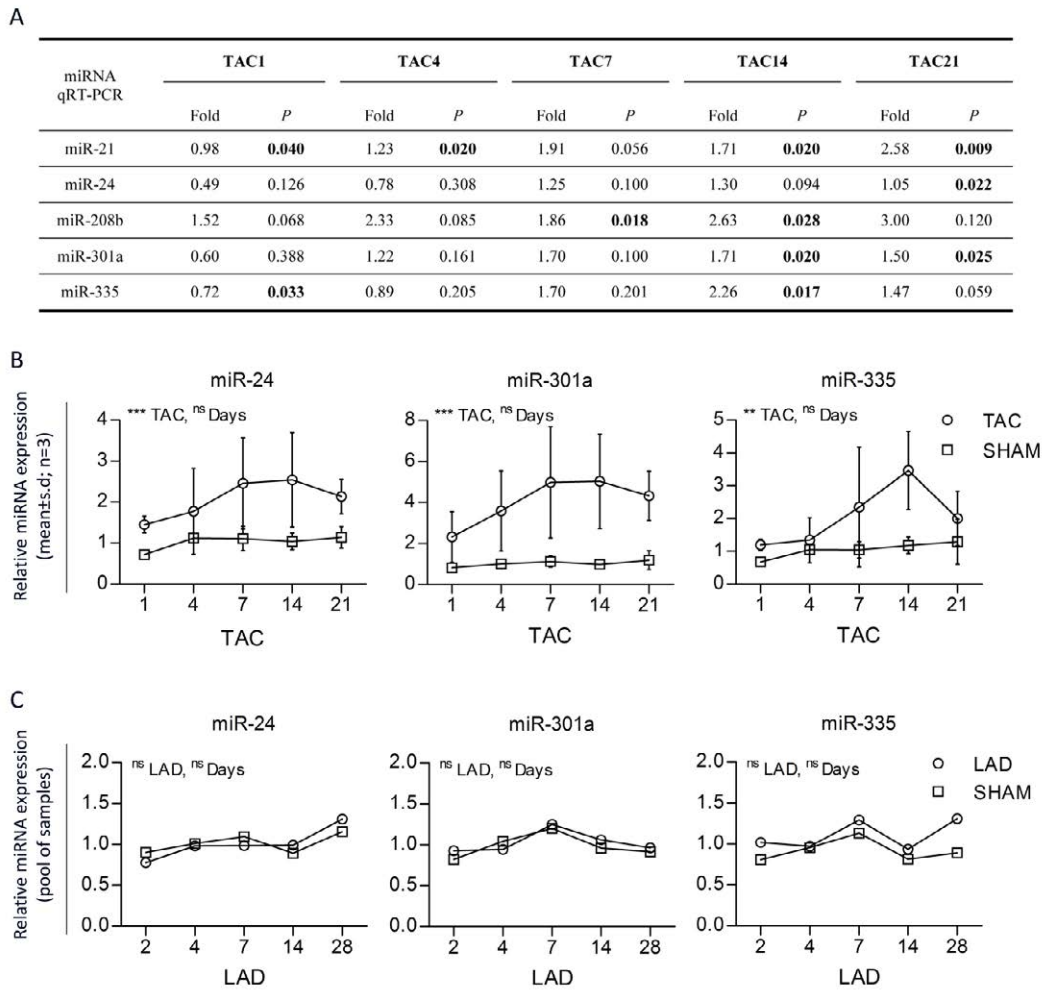


Figure 3 Verification of regulated miRNAs. (A) miR-21, miR-24, miR-208b, miR-301a and miR-335 were selected for validation using qRT-PCR. Boldface indicates significant differences from control. (B) miR-24, miR-301a and miR-335 further analyzed by comparison to SHAM operated mice. The expression level is presented mean \pm s.d, n=3. (C) Left ventricle samples from mice undergoing LAD surgery inducing MI were analyzed and showed no regulation of miR-24, miR-301a and miR-335. The expression levels were analyzed by pooling samples. Statistical significance was tested using Two-way ANOVA for significant difference over the period, * $P < 0.05$, ** $P < 0.01$ and *** $P < 0.001$.

References

- 1 Coffman TM (2011) Under pressure: the search for the essential mechanisms of hypertension. *Nat Med* 17: 1402-1409.
- 2 Van HPL, Vrints CJ, Carlier SG (2005) Coronary circulation and interventional cardiology. *Ann Biomed Eng* 33: 1735-1742.
- 3 Carabello BA, Paulus WJ (2009) Aortic stenosis. *Lancet* 373: 956-966.
- 4 Batkai S, Thum T (2012) MicroRNAs in Hypertension: Mechanisms and Therapeutic Targets. *Curr Hypertens Rep* 14: 79-87.
- 5 Olson EN (2006) Gene regulatory networks in the evolution and development of the heart. *Science* 313: 1922-1927.
- 6 van RE (2007) Control of stress-dependent cardiac growth and gene expression by a microRNA. *Science* 316: 575-579.
- 7 Care A (2007) MicroRNA-133 controls cardiac hypertrophy. *Nat Med* 13: 613-618.
- 8 van RE, Marshall WS, Olson EN (2008) Toward microRNA-based therapeutics for heart disease: the sense in antisense. *Circ Res* 103: 919-928.
- 9 Feng HJ (2014) Global microRNA profiles and signaling pathways in the development of cardiac hypertrophy. *Braz J Med Biol Res* 47: 361-368.
- 10 Bartel DP (2004) MicroRNAs: genomics, biogenesis, mechanism, and function. *Cell* 116: 281-297.
- 11 Ambros V (2004) The functions of animal microRNAs. *Nature* 431: 350-355.
- 12 Liu N (2008) microRNA-133a regulates cardiomyocyte proliferation and suppresses smooth muscle gene expression in the heart. *Genes Dev* 22: 3242-3254.
- 13 van RE (2008) Dysregulation of microRNAs after myocardial infarction reveals a role of miR-29 in cardiac fibrosis. *Proc Natl Acad Sci U S A* 105: 13027-13032.
- 14 Wang B (2012) Suppression of microRNA-29 expression by TGF-beta1 promotes collagen expression and renal fibrosis. *J Am Soc Nephrol* 23: 252-265.
- 15 Winbanks CE (2011) TGF-beta regulates miR-206 and miR-29 to control myogenic differentiation through regulation of HDAC4. *J Biol Chem* 286: 13805-13814.
- 16 Zhao YES, Srivastava D (2005) Serum response factor regulates a muscle-specific microRNA that targets Hand2 during cardiogenesis. *Nature* 436: 214-220.
- 17 Thum T (2007) MicroRNAs in the human heart: a clue to fetal gene reprogramming in heart failure. *Circulation* 116: 258-267.
- 18 Ikeda S (2007) Altered microRNA expression in human heart disease. *Physiol Genomics* 31: 367-373.
- 19 Cheng Y (2007) MicroRNAs are aberrantly expressed in hypertrophic heart: do they play a role in cardiac hypertrophy? *Am J Pathol* 170: 1831-1840.
- 20 Thum T (2008) MicroRNA-21 contributes to myocardial disease by stimulating MAP kinase signalling in fibroblasts. *Nature* 456: 980-984.
- 21 Tatsuguchi M (2007) Expression of microRNAs is dynamically regulated during cardiomyocyte hypertrophy. *J Mol Cell Cardiol* 42: 1137-1141.
- 22 Sayed D (2008) MicroRNA-21 targets Sprouty2 and promotes cellular outgrowths. *Mol Biol Cell* 19: 3272-3282.
- 23 Andersen DC (2010) MicroRNA-15a fine-tunes the level of Delta-like 1 homolog (DLK1) in proliferating 3T3-L1 preadipocytes. *Exp Cell Res* 316: 1681-1691.
- 24 Andersen DC Murine "cardiospheres" are not a source of stem cells with cardiomyogenic potential. *Stem Cells* 27: 1571-1581.
- 25 Vandesompele J (2002) Accurate normalization of real-time quantitative RT-PCR data by geometric averaging of multiple internal control genes. *Genome Biol* 3: RESEARCH0034.
- 26 Hellemans J (2007) qBase relative quantification framework and software for management and automated analysis of real-time quantitative PCR data. *Genome Biol* 8: R19.
- 27 Rockman HA (1991) Segregation of atrial-specific and inducible expression of an atrial natriuretic factor transgene in an in vivo murine model of cardiac hypertrophy. *Proc Natl Acad Sci U S A* 88: 8277-8281.
- 28 Hill JA, Olson EN (2008) Cardiac plasticity. *N Engl J Med* 358: 1370-1380.
- 29 Fiedler J (2011) MicroRNA-24 regulates vascularity after myocardial infarction. *Circulation* 124: 720-730.
- 30 Oliveira CV (2012) MicroRNAs: a new paradigm in the treatment and diagnosis of heart failure? *Arq Bras Cardiol* 98: 362-369.
- 31 Gladka MM, da Costa MPA, De Windt LJ (2012) Small changes can make a big difference - microRNA regulation of cardiac hypertrophy. *J Mol Cell Cardiol* 52: 74-82.
- 32 Qian L (2011) miR-24 inhibits apoptosis and represses Bim in mouse cardiomyocytes. *J Exp Med* 208: 549-560.
- 33 Greco S (2009) Common micro-RNA signature in skeletal muscle damage and regeneration induced by Duchenne muscular dystrophy and acute ischemia. *FASEB J* 23 : 3335-3346.
- 34 Zhou P (2012) miR-301a is a candidate oncogene that targets the homeobox gene Gax in human hepatocellular carcinoma. *Dig Dis Sci* 57: 1171-1180.
- 35 Chen Z (2012) miR-301a promotes pancreatic cancer cell proliferation by directly inhibiting Bim expression. *J Cell Biochem*.